CENTRAL ASIAN JOURNAL OF WATER RESEARCH (2024) 10(2): 1-25

https://doi.org/10.29258/CAJWR/2024-R1.v10-2/1-25.eng

Central Asian Journal of Water Research

Water Tales from Turkistan: Challenges and Opportunities for the Badam-Sayram Water System under a Changing Climate

Aidar Zhumabaev [a], Hannah Schwedhelm [b], Beatrice Marti [a], Silvan Ragettli [a], Tobias Siegfried [a]

[a] Hydrosolutions GmbH, Venusstrasse 29, 8050 Zürich, Switzerland
[b] Technical University Munich, Arcisstraße 21, 80333 Munich, Germany

ABSTRACT

The Badam River, a tributary to the Arys River located in the Syr Darya basin, is a crucial natural resource for ecological, social, and economic activities in the semi-arid region of southern Kazakhstan. The river basin is heavily influenced by manmade water infrastructure and faces water scarcity, particularly during summer, highlighting the importance of understanding its hydrological processes for effective water resource management. In this study, a semi-distributed conceptual hydrological model of the Badam River was implemented using the RS MINERVE hydrological software to evaluate the impacts of climate change on hydrology and to test the resilience of the water system. Connected HBV models were implemented for each of the hydrological response units that were defined as altitudinal zones. The hydrological model was calibrated using daily time steps between 1979 and 2011, and the resulting flow exceedance curves and hydrographs were used to assess the potential impacts of climate change on the basin, using CMIP6 precipitation and temperature scenarios. Future climate scenarios for the 2054 - 2064 period demonstrate that the peak discharge will be shifted to spring/late spring compared to the current early summer with no significant decrease in average discharge per day of the year. The insights gained from this hydrological-hydraulic model can be used to effectively manage the water system and inform future hydropower design decisions and serve as a blueprint for similar studies in the region and elsewhere.

ARTICLE HISTORY

Received: January 3, 2024
Accepted: June 6, 2024
Published: August 7, 2024

KEYWORDS

climate change, hydrological modeling, water resource, Badam-Sayram Water System, hydrological scenario analysis, decision support

CONTACT Tobias Siegfried ✉ siegfried@hydrosolutions.ch, Hydrosolutions GmbH, Venusstrasse 29, 8050 Zürich, Switzerland

Published by Kazakh German University, Almaty/Kazakhstan

1. Introduction

1.1. Background

In the semi-arid region of Central Asia, water scarcity is an ongoing challenge that causes recurrent water allocation conflicts (Bernauer & Siegfried, 2012). The Badam River basin is situated in this hydro-climatological zone and discharges via the Arys River to Syr Darya (FAO, 2012). It is a vital natural resource that supports ecological, social, and economic activities in the south of the Turkistan region of Kazakhstan (see map in Figure 1). Groundwater is used to provide drinking water (Tleuova et al., 2023).

The river emerges in the Ugam Mountain range, located on the border of Kazakhstan and Uzbekistan. The mean elevation of the basin is 965 meters above sea level (masl). The maximum and minimum elevations are 4'203 masl and 252 masl, respectively. In comparison to the other basins in the Central Asia mountainous zone of runoff formation, it is thus a very low-lying catchment (Marti et al., 2023).

The length of the river is about 141 km. The river's main tributaries are the Sayram River, Uluchur River, and the Toguz River. The river sources are springs, groundwater, snow melt, and ice melt. A significant part of the riverbed runs in gravel; therefore, it has significant losses to groundwater via filtration (Saspugaeva et al., 2019). The Badam River flows through the third largest city, Shymkent, before it joins the Arys River downstream as a left tributary. The size of the Badam catchment is 4'224 km^2, approx.

During Soviet times, two reservoirs and several diversion channels, also for interbasin water transfer from Sayram River to Badam River, were constructed. The Badam Reservoir was designed with an active capacity of 59 million cubic meters (mcm) (Scientific-Information Center of the Interstate Commission for Water Coordination of Central Asia (SIC ICWC), n.d.) to provide water for irrigation purposes downstream. The much smaller Toguz Reservoir has an active storage capacity of 4.6 mcm. It is fed by interbasin water transfer and was built to provide water for industrial purposes near Shymkent City. Due to the significant anthropogenic flow alterations, speaking about the entire Badam-Sayram Water System is adequate nowadays. The system is discussed in Section 1.2 below, and a schematic is shown in Figure 2.

With ongoing population growth in the basin, irrigation has become less important, and the role of the reservoirs in the system is changing. For example, Badam Reservoir is increasingly seen to serve recreational purposes. The provision of hydropower for the third largest city in Kazakhstan has been recognized by investors as a potentially lucrative future business. With increasingly attractive feed-in tariffs, investors are increasingly interested in developing small-scale hydropower plants (SHP). A general focus is on leveraging the hydropower potential in rivers and irrigation canals to enhance local and regional energy and water supply, considering the geopolitical, environmental, and technological contexts of Central

Asian countries and the increasing attention to transition towards a green economy (Azimov & Avezova, 2022).

The high demand for water resources in agricultural, domestic, and industrial sectors puts Kazakhstan among the countries with high water stress (Luo et al., 2013). Water stress levels are expected to increase in the 21st century (Didovets et al., 2021). Consequently, a good understanding of the hydrological processes in the basin and how these change under a changing climate is essential for effective water resource management and planning and for supporting robust hydropower developments. The climate impact study presented here contributes to this.

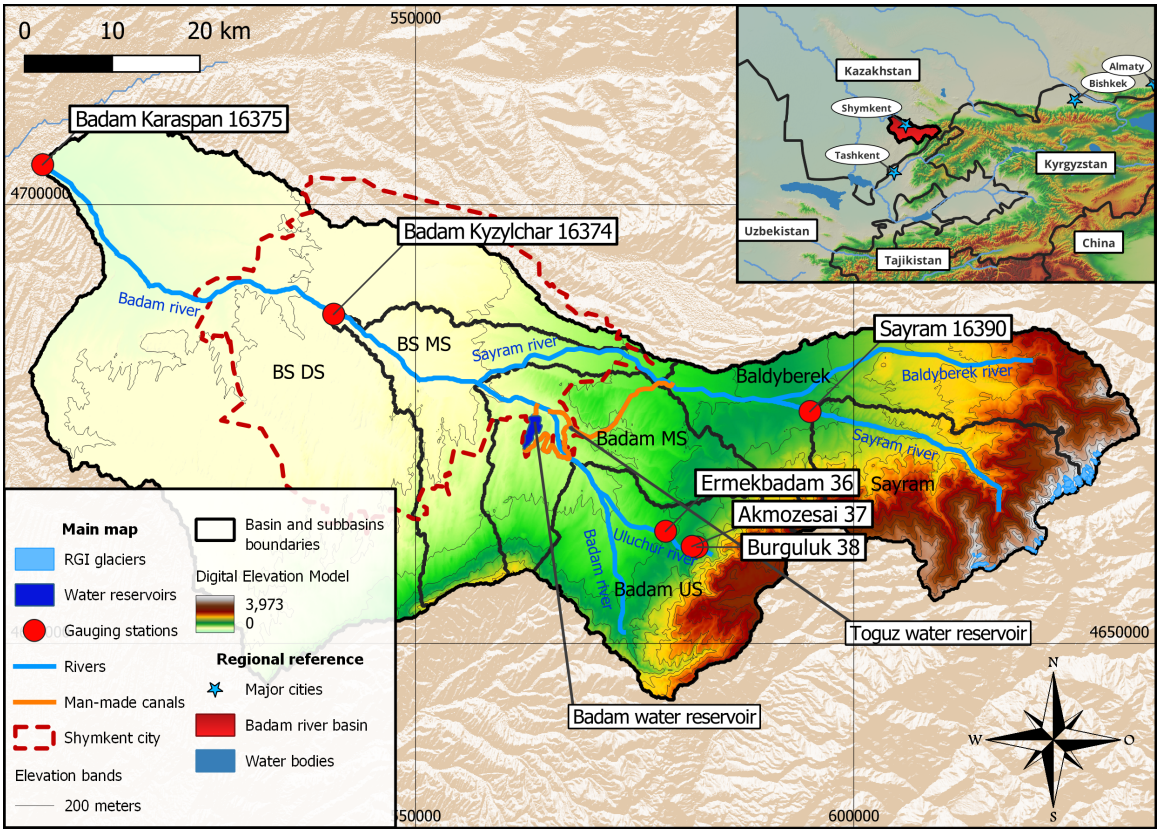

Figure 1. The map shows the study area. The base map shows the digital elevation model (DEM, SRTM (NASA JPL, 2013). The river network is given in light blue, the man-made system of diversion channels is shown in orange, and the reservoirs are in dark blue. Glacier outlines are in bright blue. The dashed line indicates the approximate boundary of Shymkent City as of 2023. The red points locate the gauging stations for which historic discharge data are available. The inlet shows the regional setting. Black solid lines indicate the basin and subbasins' boundaries with the names of the subbasins in black text. Thin black lines are elevation bands with 200 meters spacing. Numbers next to station names are station indices (KazHydromet, 2006). The background map is an ESRI hillshade layer. The map was done in QGIS (QGIS Association, 2022) with coordinates in UTM 42N (EPSG: 32642).

1.2. The Badam-Sayram Water System

This study focuses on the existing Badam-Sayram Water System (BSWS), including several diversion structures and channels, the Toguz and Badam Reservoirs. Figure 2 shows a schematic of the system, with long-term average flows in green italics. The flows in the diversion structures reflect current operating conditions and might change under different future scenarios.

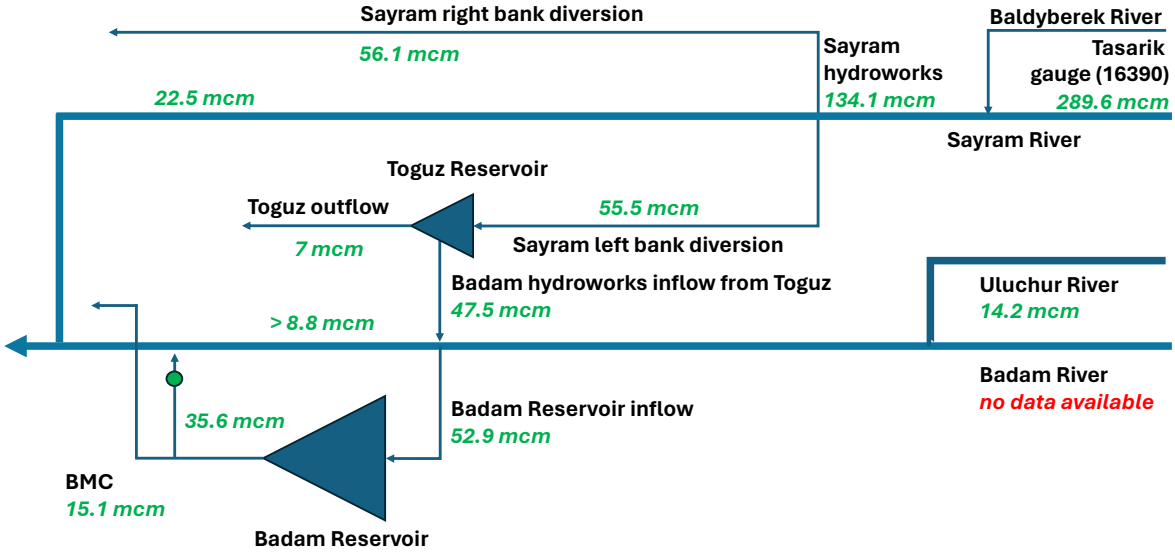

Figure 2. The BSWS schematic is shown together with the long-term water balance. Figures are in million cubic meters (mcm). Upstream Badam River discharge is ungauged. See also the map in Figure 1. BMC is the Badam Main Channel. Data have been collected from different sources, including Kazvodkhoz and the Kazakh National Meteorological and Hydrological Service (see also Table II below). The green dot indicates the location of the planned small hydropower project.

The water balance shown in Figure 2 is a long-term water balance. It shows how water from the two main tributaries, i.e., Sayram River and Badam River, gets distributed between the different diversion channels and structures. Discharge data from the upstream Badam River tributary could not be found (no data available label). It explains the estimated > 8.8 mcm flow below the Badam hydroworks as any ungauged contribution from the upstream in Badam River would need to be added here.

Between the Tasarik gauge (16390) and the inflow to Sayram hydroworks, more than half of the available flow at the gauge (5 m^3/s, approx., on average) is lost. A fraction of this is diverted into a right diversion channel for which no data is available (not shown in the schematic). It is highly likely that the bulk of this missing discharge recharges groundwater along the 16 km flow path in the coarse pebble riverbed.

In the Sayram River, the existing diversion structure at Sayram hydroworks leads water into a right-bank channel, mainly used for irrigation, and a left-bank channel. On average, 42% of the available water at the structure gets diverted to the right bank diversion channel. The left bank channel conveys water (on average, 41% of available water) towards Toguz Reservoir and Badam River. Toguz Reservoir provides water to the downstream industry. The diversion structure in the Badam River leads water from the Badam River and the additional water from the Sayram-Toguz Reservoir towards the Badam Reservoir (52.9 mcm). The 7 mcm Toguz outflow includes water used for industrial and irrigation purposes along the Sayram left bank diversion and below the Toguz Reservoir.

The water stored in and released from Badam Reservoir is used partly for irrigating agricultural and non-agricultural land near or inside the city. The difference between Badam reservoir in- and outflows, i.e. 2.2 mcm, is due to losses from evaporation over the open water surface and seepage to groundwater.

When water is released from the Badam reservoir, a fraction is diverted from the outflow into the downstream Badam Main Channel (BMC). The remaining outflow of Badam Reservoir is led back into the natural riverbed, where it is also used partly for irrigation purposes further downstream as part of the Arys River system. The water for hydroelectrical use downstream of the Badam Reservoir consists of water from the Badam River and Sayram River routed via the Toguz Reservoir. The location of the planned hydropower plant is indicated by the green dot in Figure 2.

The averaged long-term water balance shown in Figure 2 also suggests that there are ecological flows available for the ecosystems downstream of the Sayram and Badam hydroworks. It should, however, be emphasized that these annual norm values blend over possible water deficit months where the flows below the structure are much smaller or even stopped.

With the planned construction of hydropower infrastructure, the system is expected to undergo changes in the near future which will likely be reflected in a new operating regime to try to maximize hydropower output. The climate impact study presented here will help to answer the question about the resilience of the system. It will also put current and planned future operating rules in the context of changing water availability and allow reflection about eventual adjustments required.

2. Data and Methods

2.1. Data

In this study, we use various datasets to quantify climate change's impact on the hydrology of the BSWS until the mid-21st century. Table I provides a summary of the data used. Figure 4 shows a flowchart of the modeling workflow, with the corresponding data highlighted.

Table I. Summary table of key data used for the climate impact study.

Name	Description	Used for
Discharge	Monthly discharge time series from 1979 to 2011 from six gauging stations (see Table II). Source: Kazakh National Meteorological and Hydrological Service (KAZ Hydromet).	Reference data for hydrological model calibration and validation.
SRTM	Digital elevation model (DEM), 30 meters resolution, sink filled (NASA JPL, 2013).	Catchment and stream delineation and delineation of elevation bands.
CHELSA v2.1	Daily time series at 1 km grid resolution of near-surface temperature and precipitation (Karger et al., 2020, 2021).	Data from 1979 to 2011 served as baseline climate and was used for model calibration baseline and as reference period for downscaling future climate scenarios.
CMIP6	Climate change scenarios, incl. SSP1-2.6, SSP2-4.5, SSP3-7.0 and SSP5-8.5 (Riahi et al., 2017) for 3 high priority GCM, incl. GFDL-ESM4 (Krasting et al., 2018), MRI-ESM2-0 (Yukimoto et al., 2019), and UKESM1-0-LL (Tang et al., 2019).	21st century daily temperature and precipitation time series as climate scenario specific hydrological model forcing.
RGI v6.0	Glacier geometries (RGI Consortium, 2017).	Glacier geometries, geolocated, used for the computation of climate-scenario dependent glacier mass balance.
Glacier thickness	Glacier thickness data set (Farinotti et al., 2019).	Estimation of initial glacier volumes.

For model calibration and validation, monthly observations from 1979 through 2011 were used. The calibration period covered 1980 to 2000, and the validation period was from 2001 to 2011. KAZ Hydromet provided all discharge data from six gauging stations, as shown in Table II. The time span of the observational records are also indicated. The location of the gauges is shown in Figure 1.

Figure 3 shows the time series of the discharge data. Where not influenced by human activity, the seasonality shows a late spring and early summer peak discharge (Figure A1 in the Appendix shows the analysis of river discharge seasonality). This is typical for nivo-pluvial river systems in the Central Asia region (Marti et al., 2023).

Significant data gaps are apparent in the Badam Kyzylchar (16374) gauge record. The time series of Badam Karaspan shows significant changes starting at or around 1990, with a much more irregular discharge regime after that. Data measured at the Sayram Tasarik gauge (16390) shows an anomaly after the political transition at the end of 1991. The monitoring was likely impacted in the year after the demise of the Soviet Union, which would explain the anomalous data record there. Data from the Uluchur River are only available between 1979 and the end of 1991. After this, monitoring was stopped in this catchment. This prevented the use of these data for discharge calibration (see more information on the availability of high-resolution climate data below).

Table II. List of gauging stations. The gauges are sorted by ascending gauge code. See also Figure 3. The locations of the stations are shown in Figure 1. Source: KAZ Hydromet.

Gauge Name	Gauge Code	River	Norm discharge over the obs. period	Observation period
Ermekbadam	36	Uluchur River	0.5 m^3/s, 15.5 mcm	Jan. 1979 – Dec 1990
Akmozesai	37	Uluchur River	0.4 m^3/s, 12.8 mcm	Jan. 1979 – Dec 1990
Burguluk	38	Uluchur River	0.5 m^3/s, 14.2 mcm	Jan. 1979 – Dec 1990
Kyzylchar	16374	Badam River	5.9 m^3/s, 186.6 mcm	Jan. 1980 – Dec. 2020
Karaspan	16375	Badam River	9.4 m^3/s, 294.9 mcm	Jan. 1980 – Dec. 2020
Tasarik	16390	Sayram River	9.2 m^3/s, 289.6 mcm	Jan. 1980 – Dec. 2020

Comparing seasonality at Uluchur River (Burguluk Gauge) and Sayram River (Tasarik Gauge, 16390) reveals the influence of the mean catchment elevation on discharge peaks (see Figure A1 in the Appendix). Peak discharge in the Sayram catchment is one month later in June compared to the peak discharge in Uluchur, which is usually observed in May. The discharge time series from Ermekbadam shows a large anthropogenic fingerprint (upper right plates in Figure 3. From the information available to the authors, it is unclear how to explain this altered flow, which does not even show a clear seasonality).

The complex interplay between surface and groundwater in the basin must be emphasized. During a field visit, the authors could observe places of infiltration to and exfiltration from groundwater near each other. This two-way interaction between the river, its gravel bed, and the groundwater underscores the river's dynamic capability to gain and lose water, making it an important component of the catchment's hydrological cycle.

Because the records were comprehensive, data from Badam Karaspan Gauge (16375) and Sayram Tasarik (16390) were used to calibrate the hydrological model (see Chapter 2.2.3).

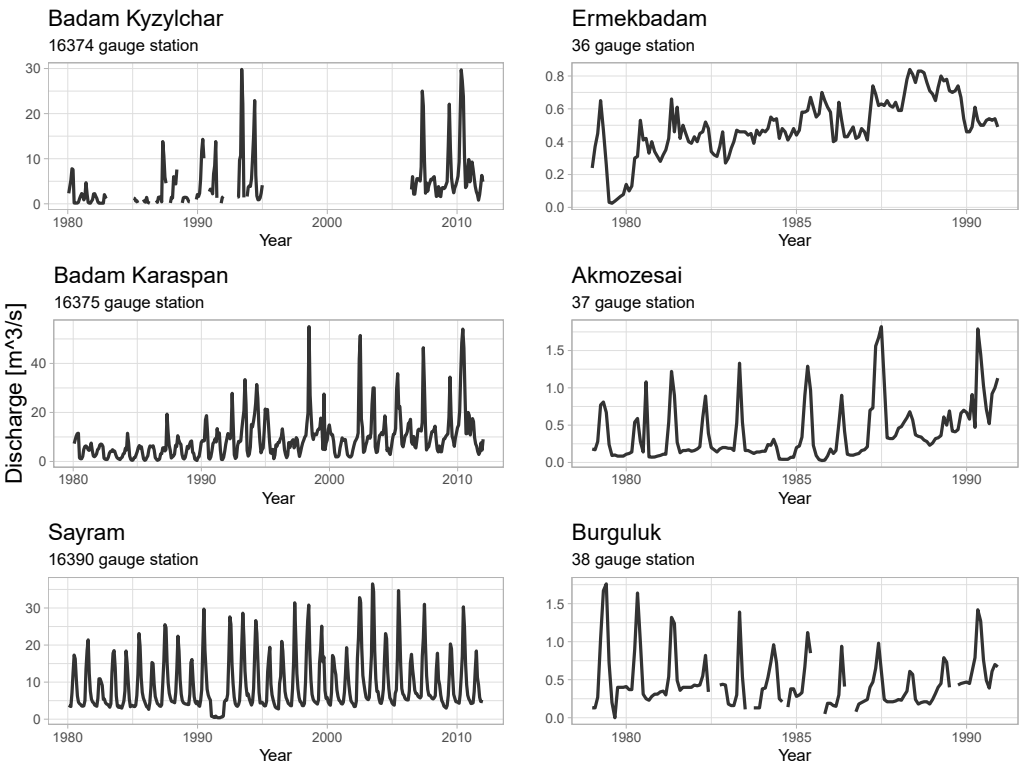

Figure 3. Mean monthly discharge time series for six gauging stations from which data was available: Badam Kyzylchar, Badam Karaspan, Sayram for 1980-2011 and Ermekbadam, Akmozesai, Burguluk for 1979-1990. See also Figure 1 for the location of gauges. Figure A1 in the Appendix shows the seasonality analysis of the gauge data.

The Shuttle Radar Topography Mission provided the digital elevation model (DEM) (NASA JPL, 2013). We used the DEM with a 30-meter spatial resolution (1 arcsec) to delineate the basin area and to define subbasins. The latter include the three upstream catchments, including the Baldyberek River, the Sayram River, and the Badam River subbasins (ordered from north to south, see Figure 1). In the Badam River catchment, an artificial gauge was introduced before the intake to the reservoir at the location of the Badam hydroworks (Figure 2). Three more subbasins were defined for the downstream, with one between Badam Karaspan and Badam Kyzylchar, the second one between Kyzylchar and the confluence between Sayram River and Badam River, and finally, this between this confluence and Badam reservoir. The DEM was used to delineate elevation bands with 200-meter vertical spacing within these subbasins.

For each elevation band, uniform near-surface temperature and precipitation time series were computed from the CHELSA v2.1 daily high-resolution climatology (Karger et al., 2020, 2021) dataset. The CHELSA v2.1 climatologies at high resolution for the earth's land surface areas are global daily climate data with a high resolution of 30 arc seconds (Karger et al., 2020, 2021).

Global products perform vastly differently when it comes to adequately reflecting the local precipitation climatologies (see, e.g. Peña-Guerrero et al., 2022). CHELSA v2.1 is based on ERA5, which we consider to be performing well in the BSWS domain. The latter is a low to medium-elevation system with four meteorological stations from the Global Historical Climatology Network daily inside or near the BSWS. The stations cover the entire elevation range and thus contribute to a reduction in uncertainties in the reanalysis data set. Station indices are: KZ000038328, UZM00038462, UZM00038339, KZ000038337, and KZ000038334 (National Centers for Environmental Information).

The advantage of near-surface CHELSA v2.1 high-resolution climatologies is that they allow for detailed analyses of climate patterns at the subbasin and elevation band levels. Furthermore, these data can be regarded as observations and thus used to downscale global circulation model outputs to study climate impacts. In this sense, these data are especially helpful in data-poor contexts such as Central Asia.

For the future climate, we obtained 21st-century daily precipitation and temperature projections from the CMIP6 project hosted by the Copernicus Climate Change Service (see https://climate.copernicus.eu). These projections are based on three different models: UKESM1.0-LL, MRI-ESM2-0, and GFDL-ESM4. The Intersectoral Impact Model Intercomparison Project standards guided the selection of GCM models. For detailed methodology, see the ISIMIP website (Lange, 2021).

Our study focuses on four combined socio-economic and climate scenarios: SSP1-2.6, SSP2-4.5, SSP3-7.0, and SSP5-8.5. These scenarios represent a range of potential future conditions based on different assumptions about greenhouse gas emissions and socio-economic developments. We used the daily climate data from these models to calculate average daily temperatures and precipitation across subbasin-specific elevation bands. This involved comparing historical data from 1979 to 2011 and bias correction using the qmap package in R to ensure accuracy (Gudmundsson et al. 2012; R Core Team 2022).

Georeferenced outlines of glaciers were provided by the Randolph Glacier Inventory (RGI Consortium, 2017). Most glacier geometries in the version V6 dataset are derived from satellite imagery (see Figure 1 for a map). We used these data in conjunction with data on glacier ice thickness (Farinotti et al., 2019) to derive initial glacier volumes and extract historical (1979 – 2011) and future climate forcing over the glaciated areas to study climate impacts on land ice and discharge in the case study basin (see Chapter 2.2.1 below).

2.2. Methods

2.2.1. Hydrological Model

Hydrological models are valuable tools for assessing a river basin's water balance and predicting the basin's response to various hydro-climatological scenarios. In recent years, hydrological models have become increasingly sophisticated, incorporating various data sources, advanced algorithms, and machine learning techniques to improve their accuracy and reliability. Here, we use a hydrological modeling approach tailored to the Central Asia region, which has proven to be applicable in the local context and yielded good results in various studies (Siegfried & Marti, 2022). Figure 4 shows the hydrological model workflow where the hydrological and hydraulic model sits at its center.

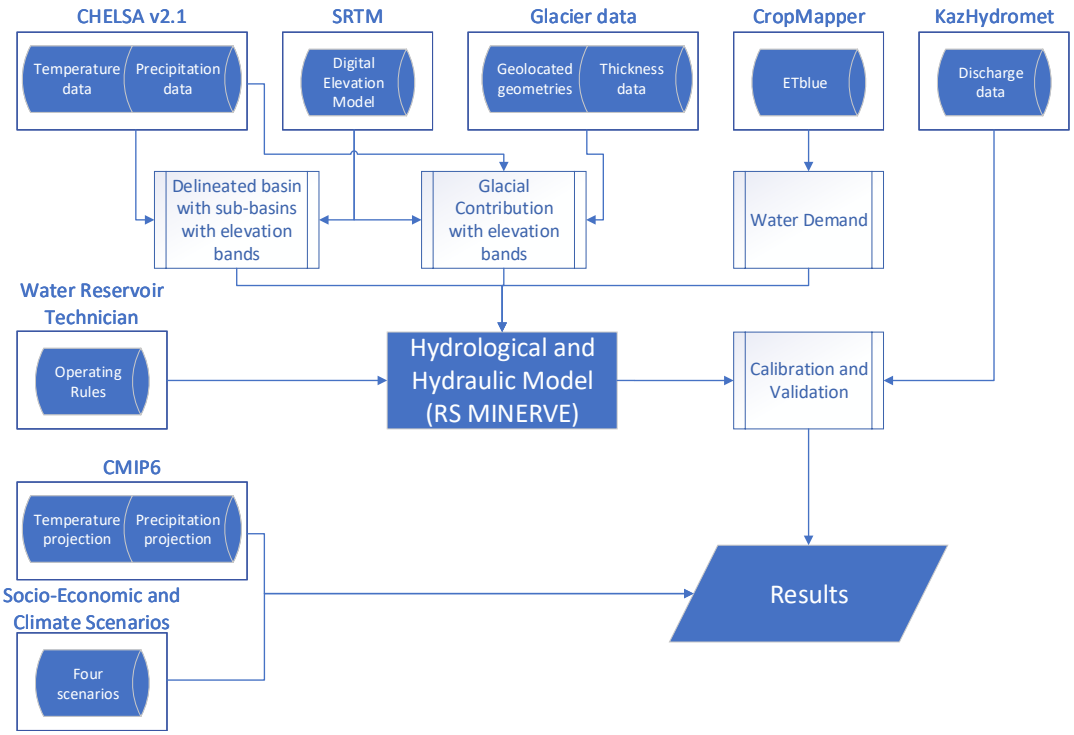

Figure 4. Flowchart for the Modelling framework. It provides a visual representation of the workflow for this study.

A semi-distributed conceptual rainfall-runoff model was implemented using the free-to-use RS MINERVE hydrological modeling environment (Foehn et al., 2020; Garcia Hernandez et al., 2020) to study climate impacts on the BSWS. RS MINERVE is a hydrological modeling software developed by the CREALP - Research Centre on Alpine Environment, in collaboration with the Swiss Federal Institute of Technology in Lausanne, the Polytechnic University of Valencia, and the company Hydro10 (RS Minerve, 2021). This software is designed to support the analysis and management of water resources through comprehensive simulation capabilities. It utilizes hydrological and hydraulic models that can be interlinked and applied to watersheds, rivers, and reservoir systems to study water flow dynamics. Additionally, RS MINERVE provides a user-friendly interface (see Figure A2) and graphical tools for modeling, which facilitate the visualization and interpretation of hydrological data and simulation results. In this study, RS MINERVE is utilized to implement a semi-distributed conceptual model with subbasins and elevation bands.

The river basin was divided into six subbasins with corresponding elevation bands to adequately represent the elevation-dependent dynamics of snow melt and snow accumulation at sub-annual scales. Separate HBV models (Bergström, 1976) were implemented for each elevation band in each subbasin. The HBV model consists

of a snowpack, a water content reservoir, a soil humidity reservoir, and upper and lower soil storage reservoirs. Within this framework, each model is configured with 15 calibratable parameters that control the various processes. The area of the subbasin, being a fixed geographic attribute, was not calibrated because it serves as a static parameter within the model. This parameter of an area of subbasin ensures that the physical characteristics of the subbasin are accurately represented while allowing the dynamic hydrological processes to be fine-tuned during calibration. Like this, 57 HBV models were set up in total and interlinked (Figure A2 in the Appendix).

Model zonation was introduced to avoid over-parameterization, and three zones were defined according to either upstream, midstream, or downstream elevation band or HBV model location. The zonation was motivated by the subbasin characteristics determined by the underlying geology, with plutonic rocks dominating the upstream and mixed sedimentary rocks and unconsolidated sediments prevalent in the mid- and downstream of the BSWS (Hartmann & Moosdorf, 2012). The parameters of the HBV models grouped in one zone share all the same parameter values. The calibrated final parameter values are shown in the Appendix in Table A1. The model calibration and validation process is described in Section 2.2.3, and the results are presented in Section 3.

The HBV models model liquid water and solid water stored as snow. Glacier contributions to discharge needed to be implemented outside the HBV model components and were added separately as source terms to each subcatchment discharge where glaciers are present. For this purpose, we set up a daily glacier mass balance model for each glacier in the Badam River. Glacier mass loss is simulated on individual elevation bands of 100 m intervals using temperature and precipitation forcing from the CHELSA v2.1 data set. Per-glacier melt was implemented with a degree-day glacier melt model (Hock, 2003) that was calibrated against simulated glacier ablation rates derived from Miles et al. (2021) and Hugonnet et al. (2021).

The glacier area-volume scaling by Erasov (Erasov, 1986) was fitted with glacier areas and volumes derived from the RGI data set and the glacier thickness estimates by Farinotti et al. (2019). The glacier contributions were computed in R and added as source elements for each upstream catchment with glaciation, i.e., Baldyberek River and Sayram River. The future land ice dynamics were computed similarly with the bias-corrected daily GCM- and climate scenario-specific temperature and precipitation forcings determining the future mass balance components.

2.2.2. Modeling Hydraulic Structures and Water Demand

The infrastructure elements in the BSWS were implemented using corresponding hydraulic model elements in RS MINERVE. For an overview of these elements, see (Garcia Hernandez et al., 2020). We differentiate between manmade diversion and storage infrastructure on the one hand and locations for water demand on the other.

The two reservoirs in the basin were implemented as RS MINERVE reservoir objects. Each reservoir has an associated level-discharge relationship (HQ) object. HQ objects for reservoir discharge were implemented since reservoir operating rules were unavailable. This allowed us to mimic a mean operational regime without precise knowledge of the operating rules.

In conjunction with kinematic wave objects, structure efficiency objects were chosen to account for water diversions in canals to and from the reservoirs. Values were chosen following local feedback (personal communication with A. Urazkeldiev). The design specifics of the reservoirs and the canals were obtained from personal communication with on-the-ground staff from Badam hydroworks during a field visit in October 2021 and during follow-up conversations.

We used unsupervised classification to map irrigated land in the BSWS (Ragettli et al., 2018). For the crop disaggregated mapping, we used the freely available CropMapper application (Silvan Ragettli, 2022). A total area of 294 km^2 was mapped as irrigated land. It corresponds to approximately 7% of the total basin area. Four dominant crop classes were identified, and annual evaporation from irrigation water (ETblue) was computed for each crop class and each subbasin. The different crop types are used to estimate the mean ETblue component over the entire domain. The following values were determined for each crop class via the CropMapper: cotton 391 mm/a, winter wheat 292 mm/a, rice 686 mm/a, and unknown 489 mm/a. The crop class unknown encompasses all classes that could not be further disaggregated. Table III summarizes the derived mean annual water demand in terms of volumes over the corresponding crop areas.

Table III. Mean annual irrigation water demand in the subbasins of the BSWS. All numbers are in million cubic meters (mcm), which is equivalent to gigaliters (gl). BS MS is Badam-Sayram River midstream, and BS DS Badam-Sayram downstream. Badam US and Badam MS are the corresponding sections of the Badam River before its confluence with Sayram River (see Figure 1). The column Total shows the sum over all subbasins.

Crop Class	Total	Baldyberek	Sayram	Badam US	Badam MS	BS MS	BS DS
Cotton	6.2	0.1	0.6	1.7	0.8	0.3	2.6
Winter wheat	18.5	0.7	1.5	10.1	4.7	0.1	1.2
Rice	17.7	1.0	4.5	3.6	3.4	1.6	3.7
Unknown	20.7	1.5	5.6	4.0	3.7	1.8	4.1
Total	63.1	3.3	12.3	19.4	12.7	3.8	11.6

For each subbasin, we implemented an RS MINERVE consumer object (see also Figure A2 in the Appendix). We mimicked seasonal irrigation water demand by uniformly distributing the total demand for each subbasin, as shown in Table III, throughout the irrigation season, i.e., from April through the end of September. During the cold season, we assume that the consumer object demand is equal to 0. For the future climate scenarios, we assumed that total seasonal water demand would remain unchanged over the course of the 21st century. This rests on the assumption that an increasing atmospheric water demand from increases in surface temperatures and an associated increase in ETblue would be offset by a reduced size of the irrigated area due to continued land pressure from urbanization.

2.2.3. Model Calibration and Validation

The hydrological model was run with daily time steps to simulate historical and future climate scenario-dependent discharge. A screenshot of the hydrological-hydraulic model is provided in the Appendix in Figure A2. The two gauges, Sayram Tasarik (16390) and Badam Karaspan (16375) were used for parameter calibration from 1979 to 2000 and validation from 2001 to 2011. For calibration, the built-in Shuffled Complex Evolution Algorithm was used (SCE-UA). The SCE-UA algorithm is a global optimization technique that uses a combination of deterministic and stochastic processes to efficiently explore and exploit multidimensional search spaces, enhancing the performance of model calibration by evolving a population of solutions through competitive evolution and systematic recombination (Duan et al., 1992). Results are discussed in Section 3.

3. Results

Calibration results are shown in Figure 5. The Nash-Sutcliffe model efficiency (NSE) coefficient is 0.3831 for the validation period at Gauge Badam Karaspan 16375 and 0.4511 at Gauge Sayram 16390. The NSE coefficient is a statistical tool used to assess the predictive power of hydrological models (Nash & Sutcliffe, 1970). The NSE quantifies how well the plot of observed versus simulated data fits. It ranges from negative infinity to 1. An NSE of 1 indicates a perfect match between model simulations and observations, representing an ideal model. Where NSE is less than 0, the observed mean discharge is better than the model.

As Figure 5 shows, the model nicely captures the seasonality of discharge and the interannual variability. Given the complexity of the BSWS, we consider the model's performance satisfactory. The model is now ready for use in a climate impact assessment.

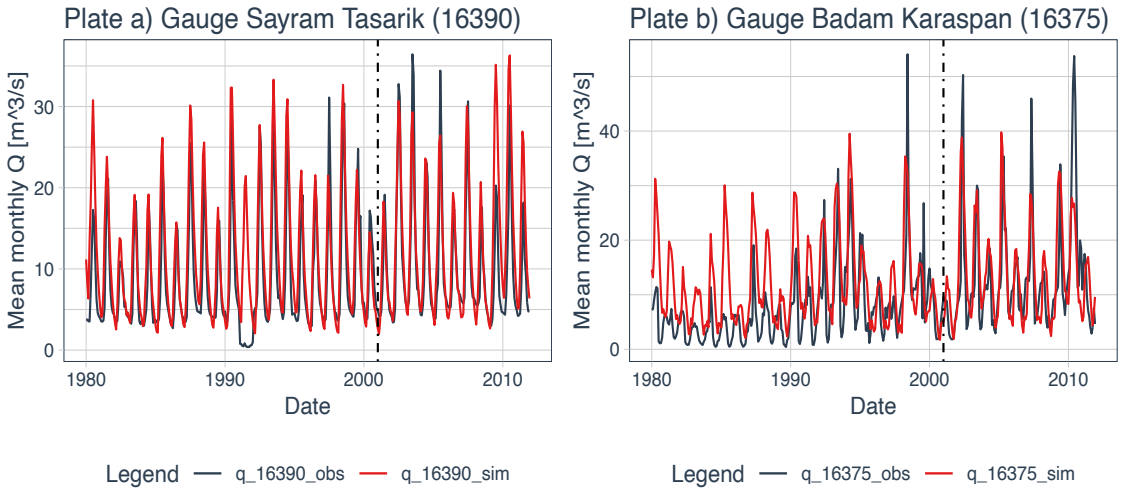

Figure 5. Comparison of observed mean monthly discharge data (black) with simulation results (red) for Sayram Gauge 16390 (Plate a) and Badam Karaspan Gauge 16375 (Plate b). The dotted vertical lines indicate the dividers between calibration and validation sets.

The two plates in Figure 6 show flow duration curves for the Sayram River and Badam River upstream of the diversion structures, right at the corresponding intake points, respectively. Flow duration curves show the cumulative number of days per year when the discharge exceeds a certain threshold (Bedient et al., 2013). Discharge is measured in cubic meters per second (m^3/s), and the x-axis represents time in days per year.

The plates compactly compare the current climate discharge with projections under different climate scenarios for 2054 – 2064. The target horizon was chosen to cover the typical lifetime of a hydropower infrastructure installation, such as the one studied under the Badam Reservoir Hydro4U feasibility study (Schwedhelm, 2023). The dashed lines represent the historical river discharge simulation for the 1979 – 2011 baseline period at the particular locations. They serve as the baseline for comparison with future scenarios. The solid lines represent the average (mean) discharge under the four climate scenarios (SSP1-2.6, SSP2-4.5, SSP3-7.0, SSP5-8.5).

The curves generally follow a similar pattern, where discharge is higher for fewer days and gradually decreases. At Sayram River (left plate, Figure 6), the projected discharge under the SSP3-7.0 scenario is less than the historical discharge for a significant portion of the year (green line), indicating a possible decrease in water availability. Other scenarios at Sayram River show discharges like those for most days compared to historical simulations. Badam river curves under all future scenarios appear to follow a very close pattern, with minimal differences between the scenarios, except SSP5-8.5, which has more discharge than the current climate.

These results suggest that the impact of different climate scenarios on the average discharge in the basin might be relatively moderate over the studied time horizon. This finding is confirmed by regional climate impact studies (see, e.g., Siegfried et al., 2023).

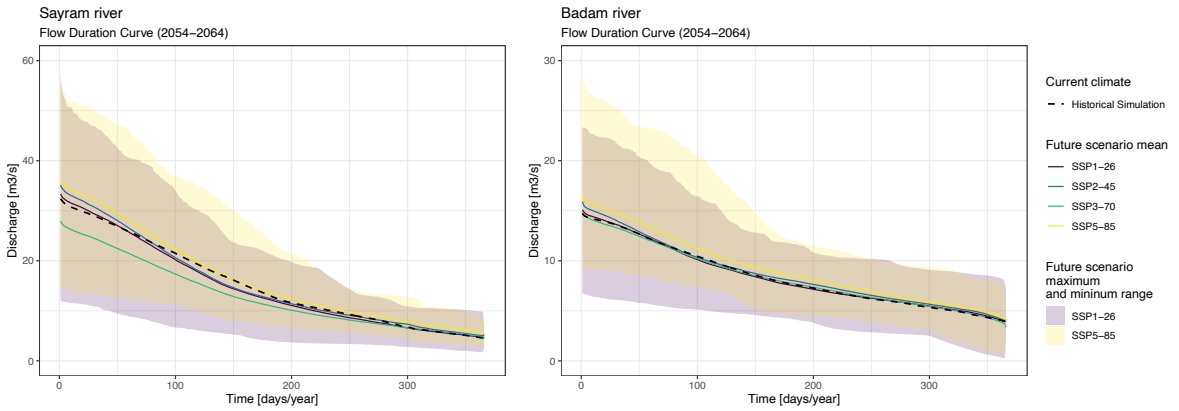

Figure 6. Simulated exceedance curves for the Sayram River upstream of the diversion to Toguz Reservoir (left plate) and Badam River upstream of the diversion to Badam Reservoir (right plate). The curves are computed for the river flow right at the corresponding intake points. The dashed lines are the exceedance curves for the baseline period from 1979 – 2011. The climate scenario-dependent curves are shown accordingly for the period 2054 – 2064.

To study the impact of climate change on discharge in terms of changes in the intra-annual distribution of discharge, we investigate changes to monthly discharge values at Badam Kyzylchar. The gauge is in the center of Shymkent city and thus is a good point for studying the changing availability of renewable water resources for the BSWS. The results for the SSP3-7.0 scenario are shown in Figure 7 for the simulated 2011 – 2070 period with 60 years of data available. The results are GCM-model averaged monthly values.

Positive sloped regression lines for individual months indicate an increasing discharge trend for the month under consideration. Conversely, negative sloped lines indicate declining trends. Strongly increasing December to May discharge trends are visible where increases in monthly mean discharge of + 20 % are modeled. A slightly declining water availability is observed during the July and August months. It should be noted that the results are comparable for the SSP1-2.6, SSP2-4.5, and SSP5-8.5 scenarios.

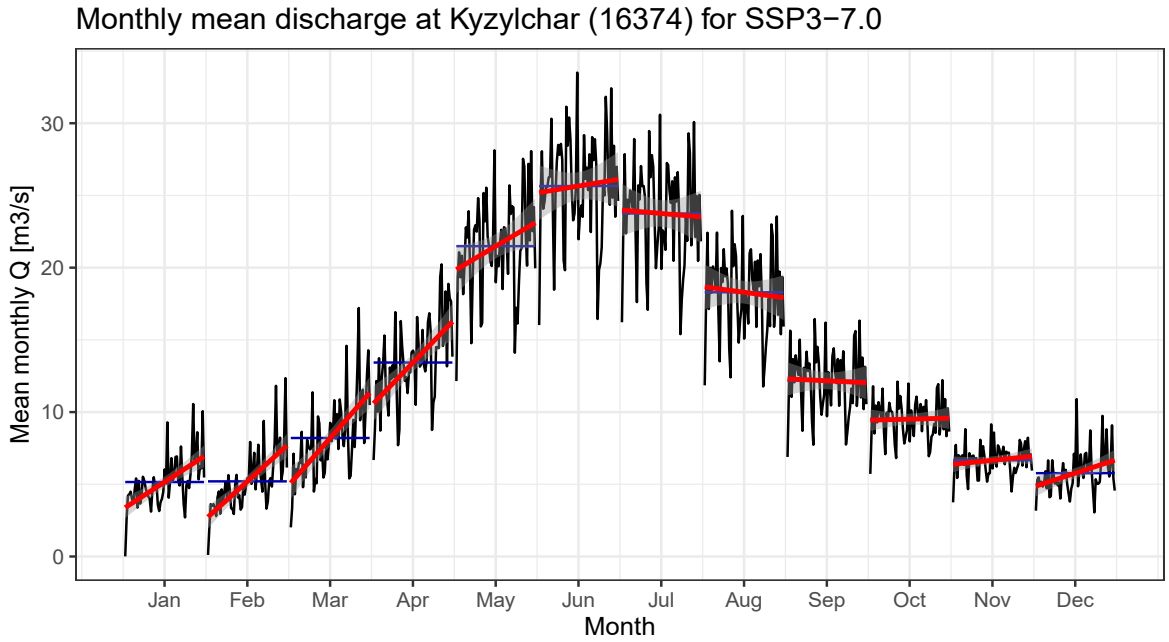

Figure 7. Changes in the future monthly mean discharge under the SSP3-7.0 scenario at Badam Kyzylchar. The simulated period is from 2011 – 2070. All monthly data are binned in their corresponding month (black lines). The red lines show simple regression lines for each month separately. The blue lines are average monthly values taken over the entire period.

4. Discussion

The hydrological modeling of the BSWS, undertaken in this study, offers valuable insights into the water dynamics of a basin crucial for the ecological, social, and economic fabric of the Turkistan area in southern Kazakhstan. The semi-distributed conceptual rainfall-runoff model implemented has enabled a detailed analysis of the basin's response to climatic variables, showcasing the intricate interplay between natural processes and anthropogenic factors. It is also important to support decisions in the context of an increasingly interconnected world and Water-Energy-Food-Climate Nexus considerations (De Keyser et al., 2023).

The observed data highlight a seasonal variability in discharge, with peak flows occurring during the spring and early summer months. This pattern is consistent across all gauging stations and indicates snowmelt and spring rains' significant influence on the runoff generation processes. The forward-looking aspect of this study, utilizing future climate scenarios, provides a glimpse into the potential impacts of climate change on the hydrology of the BSWS. As indicated by the model, the shift in peak discharge timings raises concerns about the timing and availability of water resources

at intra-annual time scales, particularly during the high-demand summer months (see Figure 7). This temporal shift may lead to mismatches between water supply and demand, with significant implications for agriculture, industry, and domestic water supply. However, the BSWS can be considered climate resilient because there is active storage that can be managed in the basin and because we do not expect to see a declining water availability over the studied time horizon. The reservoirs in the BSWS can help to address the changing seasonality issue through changes in the storage management of existing or future reservoirs.

There is a clear need for continuous monitoring of the basin's hydrology to validate and refine the model. Integrating new datasets, such as high-resolution satellite imagery and monitoring data, could significantly enhance the model's predictive capabilities. Daily snow water equivalent estimates provided by the High Mountain Asia Snow Reanalysis product at a 500-meter grid resolution could improve model calibration to address the paucity of in-situ data (Liu et al., 2021). Furthermore, research into the socioeconomic impacts of changing water availability on local communities could provide a more holistic understanding of the basin's future under various climate scenarios.

The influence of human activities on the hydrological regime is evident, with the operation of water reservoirs and proposed hydropower developments indicating a substantial anthropogenic footprint in the river basin. The dual-purpose use of the reservoirs for agriculture and recreation and the studied interventions under the Hydro4U project illustrate the complexities of water resource management in the region.

While the modeling approach chosen to study climate impacts on the BSWS is considered adequate for this purpose, it has limitations. One such limitation is the model's inability to accurately replicate the gravel riverbed's filtration dynamics (groundwater), an essential component of the hydrological cycle in the area. This gap highlights the need for further research into the catchment's subsurface hydrology and the potential for improved modeling techniques to capture these processes better. The need for this is further accentuated by the fact that groundwater contamination threatens drinking water supplies for the fast-growing Shymkent city and its environs. Substantial contaminations of nitrate, phosphate, phosphorous, fluoride, and lead are already detected (Tleuova et al., 2023).

The research provides a foundation for informed decision-making in managing the BSWS resources. It also helps in the proper design of hydropower infrastructure. As climate change continues to reshape hydrological regimes globally, the lessons gained here can inform similar studies in semi-arid regions worldwide, highlighting the critical role of integrated hydrological-hydraulic modeling studies in sustainable water resource management.

5. Conclusion

The study examines the impact of climate change on the hydrology of the Badam River basin, a critical water resource in southern Kazakhstan. The research question focuses on how climate change affects water availability and hydrological processes in this semi-arid region. For this, we have implemented a semi-distributed conceptual hydrological model using the RS MINERVE software, with calibration based on historical data from 1979 to 2011 and projections for 2054-2064 using CMIP6 climate scenarios.

The findings indicate that peak discharges will shift from early summer to late spring, but the mean availability of renewable water resources is not expected to change dramatically in the BSWS until the 2054 – 2064 period. From this perspective, we consider the BSWS to be climate resilient. It also means that the development of SHP remains an attractive option over the studied time horizon, thus contributing to the green energy transition of the Central Asia region.

The main driver of change in the BSWS will be the socio-economic and population development in the basin, with population increases following or surpassing the country-level UN Population projections for Kazakhstan (United Nations Department of Economic and Social Affairs Population Division, 2022).

Water needs for recreational purposes, drinking, and industrial processes will increase accordingly, further putting pressure on ecosystems. Water for irrigation in the basin will likely further decline as Shymkent city grows. Finally, non-consumptive water use for hydropower production will likely increase energy-water linkages. These developments have significant policy and system management implications and might require upgrading the system to increase storage.

Under any circumstances, the future regulatory focus should shift toward maintaining and augmenting water quality to ensure a good status of the aquatic systems and to ensure drinking water quality is according to required quality standards. This also means that the connection between surface and groundwater needs to be acknowledged explicitly, and the understanding of the interconnectedness of these resources needs to be further improved. This should include establishing a comprehensive monitoring program for surface and groundwater, including quantity and quality. This new data could also be used to improve hydrological-hydraulic models, such as the one presented here.

As we look into the future, it is evident that integrated hydrological studies, continuous monitoring, and transboundary cooperation will be the keystones for navigating the uncertainties of a changing world. The BSWS, with its complex interplays of natural processes and human interventions, offers a case study that can inform similar hydrological assessments and water management strategies across semi-arid regions around the globe.

Research Funding

This research has received funding from the European Union's Horizon 2020 research and innovation programme under grant agreement No 101022905.

Acknowledgments

We thank the Kazakh National Meteorological and Hydrological Service for providing data on discharge. Additionally, thanks are to Abdikhamid Urazkeldiyev and Oyture Anarbekov, whose assistance and consultancy during the fieldwork were invaluable.

References

Azimov, U., & Avezova, N. (2022). Sustainable small-scale hydropower solutions in Central Asian countries for local and cross-border energy/water supply. *Renewable and Sustainable Energy Reviews*, 167, 112726. https://doi.org/10.1016/j.rser.2022.112726

Bedient, P. B., Huber, W. C., & Vieux, B. E. (2013). Hydrology and Floodplain Analysis. *Prentice Hall*. https://books.google.ch/books?id=53JBpwAACAAJ

Bergström, S. (1976). Development and application of a conceptual runoff model for Scandinavian catchments (RHO, *Hydrology and Oceanography,* ISSN 0347-7827 ; 7, p. p.162).

Bernauer, T., & Siegfried, T. (2012). Climate change and international water conflict in Central Asia. *Journal of Peace Research*, 49(1), 227–239. https://doi.org/10.1177/0022343311425843

De Keyser, J., Hayes, D. S., Marti, B., Siegfried, T., Seliger, C., Schwedhelm, H., Anarbekov, O., Gafurov, Z., López Fernández, R. M., Ramos Diez, I., Alapfy, B., Carey, J., Karimov, B., Karimov, E., Wagner, B., & Habersack, H. (2023). Integrating Open-Source Datasets to Analyze the Transboundary Water-Food-Energy-Climate Nexus in Central Asia. *Water,* 15(19). https://doi.org/10.3390/w15193482

Didovets, I., Lobanova, A., Krysanova, V., Menz, C., Babagalieva, Z., Nurbatsina, A., Gavrilenko, N., Khamidov, V., Umirbekov, A., Qodirov, S., Muhyyew, D., & Hattermann, F. F. (2021). Central Asian rivers under climate change: Impacts assessment in eight representative catchments. *Journal of Hydrology: Regional Studies*, 34, 100779. https://doi.org/10.1016/j.ejrh.2021.100779

Duan, Q., Sorooshian, S., & Gupta, V. (1992). Effective and efficient global optimization for conceptual rainfall-runoff models. *Water Resources Research,* 28(4), 1015–1031. https://doi.org/10.1029/91wr02985

Erasov, N. V. (1986). Method for determining of volume of mountain glaciers. *Mater. Glyatsiol.*, 14, 307–308.

FAO. (2012). AQUASTAT Transboundary River Basin Overview – Aral Sea. *Food and Agricultural Organization of the United Nations* (FAO).

Farinotti, D., Huss, M., Fürst, J. J., Landmann, J., Machguth, H., Maussion, F., & Pandit, A. (2019). A consensus estimate for the ice thickness distribution of all glaciers on Earth. *Nature Geoscience,* 12(3), 168–173. https://doi.org/10.1038/s41561-019-0300-3

Foehn, A., Garcia Hernandez, J., Roquier, B., Fluixa-Sanmartin, J., Brauchli, T., Paredes Arquiola, J., & De Cesare, G. (2020). RS MINERVE - *User Manua*l, V2.15 (ISSN 2673-2653). Ed. CREALP.

Garcia Hernandez, J., Foehn, A., Fluixa-Sanmartin, J., Roquier, B., Brauchli, T., Paredes Arquiola, J., & G, D. C. (2020). RS MINERVE - *Technical manual,* v2.25 (ISSN 2673-2661). Ed. CREALP.

Gudmundsson, L., Bremnes, J. B., Haugen, J. E., & Engen-Skaugen, T. (2012). Technical Note: Downscaling RCM precipitation to the station scale using statistical transformations – a comparison of methods. *Hydrology and Earth System Sciences*, 16(9), 3383–3390. https://doi.org/10.5194/hess-16-3383-2012

Hartmann, J., & Moosdorf, N. (2012). The new global lithological map database GLiM: A representation of rock properties at the Earth surface. *Geochemistry, Geophysics, Geosystems*, 13(12). https://doi.org/10.1029/2012GC004370

Hock, R. (2003). Temperature index melt modelling in mountain areas. *Journal of Hydrology*, 282(1-4), 104–115. https://doi.org/10.1016/S0022-1694(03)00257-9

Hugonnet, R., McNabb, R., Berthier, E., Menounos, B., Nuth, C., Girod, L., Farinotti, D., Huss, M., Dussaillant, I., Brun, F., & Kääb, A. (2021). Accelerated global glacier mass loss in the early twenty-first century. *Nature*, 592(7856), 726–731. https://doi.org/10.1038/s41586-021-03436-z

Karger, D. N., Schmatz, D. R., Dettling, G., & Zimmermann, N. E. (2020). High-resolution monthly precipitation and temperature time series from 2006 to 2100. *Scientific Data*, 7(1), 248. https://doi.org/10.1038/s41597-020-00587-y

Karger, D. N., Wilson, A. M., Mahony, C., Zimmermann, N. E., & Jetz, W. (2021). Global daily 1 km land surface precipitation based on cloud cover-informed downscaling. *Scientific Data*, 8(1), 307. https://doi.org/10.1038/s41597-021-01084-6

KazGidromet [KazHydromet]. (2006). Gosudarstvennyj Vodnyj Kadastr Respubliki Kazahstan: Mnogoletnie dannye o rezhime i resursah poverhnostnyh vod sushi. Vypusk 3 [State Water Cadastre of the Republic of Kazakhstan: Long-term data on the regime and resources of land surface waters. Issue 3]. Ministersvo Ohrany Okruzhajushhej Sredy [Ministry of Environmental Protection]. (in Russian)

Krasting, J. P., John, J. G., Blanton, C., McHugh, C., Nikonov, S., Radhakrishnan, A., Rand, K., Zadeh, N. T., Balaji, V., Durachta, J., Dupuis, C., Menzel, R., Robinson, T., Underwood, S., Vahlenkamp, H., Dunne, K. A., Gauthier, P. P., Ginoux, P., Griffies, S. M., … Zhao, M. (2018). NOAA-GFDL GFDL-ESM4 model output prepared for CMIP6 CMIP. *Earth System Grid Federation*. https://doi.org/10.22033/ESGF/CMIP6.1407

Lange, S. (2021). ISIMIP3b bias adjustment fact sheet. https://www.isimip.org/documents/413/ISIMIP3b_bias_adjustment_fact_sheet_Gnsz7CO.pdf

Liu, Y., Fang, Y., & Margulis, S. (2021). High Mountain Asia UCLA Daily Snow Reanalysis [dataset]. *NASA National Snow and Ice Data Center DAAC*. https://doi.org/10.5067/HNAUGJQXSCVU

Luo, T., Young, R., & Paul, R. (2013). Aqueduct country and river basin rankings: A weighted aggregation of spatially distinct hydrological indicators. *Washington, DC: World Resources Institute*. https://www.wri.org/research/aqueduct-country-and-river-basin-rankings

Marti, B., Yakovlev, A., Karger, D. N., Ragettli, S., Zhumabaev, A., Wakil, A. W., & Siegfried, T. (2023). CA-discharge: Geo-Located Discharge Time Series for Mountainous Rivers in Central Asia. *Scientific Data*, 10(1), 579. https://doi.org/10.1038/s41597-023-02474-8

Miles, E., McCarthy, M., Dehecq, A., Kneib, M., Fugger, S., & Pellicciotti, F. (2021). Health and sustainability of glaciers in High Mountain Asia. *Nature Communications*, 12(1), 2868. https://doi.org/10.1038/s41467-021-23073-4

National Centers for Environmental Information. Daily Observational Data. (https://www.ncei.noaa.gov/maps/daily/)

NASA JPL. (2013). NASA Shuttle Radar Topography Mission Global 1 arc second [Data set]. *NASA EOSDIS Land Processes DAAC*. https://doi.org/10.5067/MEaSUREs/SRTM/SRTMGL1.003

Nash, J. E., & Sutcliffe, J. V. (1970). River flow forecasting through conceptual models part I — A discussion of principles. *Journal of Hydrology*, 10(3), 282–290. https://doi.org/10.1016/0022-1694(70)90255-6

Peña-Guerrero, M. D., Umirbekov, A., Tarasova, L., & Müller, D. (2022). Comparing the performance of high-resolution global precipitation products across topographic and climatic gradients of Central Asia. *International Journal of Climatology*, 42(11), 5554–5569. https://doi.org/10.1002/joc.7548

QGIS Association. (2022). QGIS Geographic Information System [Computer software]. QGIS.org. http://www.qgis.org

Ragettli, S., Herberz, T., & Siegfried, T. (2018). An Unsupervised Classification Algorithm for Multi-Temporal Irrigated Area Mapping in Central Asia. *Remote Sensing*, 10(11), 1823. https://doi.org/10.3390/rs10111823

RGI Consortium. (2017). Randolph Glacier Inventory – A Dataset of Global Glacier Outlines: Version 6.0 [dataset]. https://doi.org/che

Riahi, K., van Vuuren, D. P., Kriegler, E., Edmonds, J., O'Neill, B. C., Fujimori, S., Bauer, N., Calvin, K., Dellink, R., Fricko, O., Lutz, W., Popp, A., Cuaresma, J. C., Kc, S., Leimbach, M., Jiang, L., Kram, T., Rao, S., Emmerling, J., … Tavoni, M. (2017). The Shared Socioeconomic Pathways and their energy, land use, and greenhouse gas emissions implications: An overview. *Global Environmental Change*, 42, 153–168. https://doi.org/10.1016/j.gloenvcha.2016.05.009

RS Minerve (2.9.1). (2021). [Computer software]. CREALP. https://crealp.ch/rs-minerve/

Saspugaeva, G. E., Mahambetova, N. M., Ramazanova, N. E., & Tulebekova, A. S. (2019). Jekologicheskie problemy vodnyh resursov Juzhno-Kazahstanskoj oblasti [Ecological problems of water resources of South Kazakhstan region]. *Vestnik Vostochno-Kazahstanskogo Gosudarstvennogo Tehnicheskogo Universiteta Im. D. Serikbaeva* [Bulletin of the East Kazakhstan State Technical University Named after D. Serikbaev], № 2, C. 51-55. (in Russian)

Schwedhelm, H. (2023). Feasibility Study Badam Reservoir.

Scientific-Information Center of the Interstate Commission for Water Coordination of Central Asia (SIC ICWC). (n.d.). *Portal of Knowledge for Water and Environmental Issues in Central Asia*. www.Cawater-Info.Net. http://www.cawater-info.net/bk/1-1-1-1-3-kz_e.htm

Siegfried, T., & Marti, B. (2022). Modeling of Hydrological Systems in Semi-Arid Central Asia. GitHub Pages. https://doi.org/10.5281/zenodo.4666499

Siegfried, T., Mujahid, A. U. H., Marti, B., Molnar, P., Karger, D. N., & Yakovlev, A. (2023). Unveiling the Future Water Pulse of Central Asia: A Comprehensive 21st Century Hydrological Forecast from Stochastic Water Balance Modeling. https://doi.org/10.21203/rs.3.rs-3611140/v1

Silvan Ragettli. (2022). Remote Sensing and Geospatial Analysis Applied to Irrigation Performance Assessment, *CropMapper Methodology* (01.03.2022).

Tang, Y., Rumbold, S., Ellis, R., Kelley, D., Mulcahy, J., Sellar, A., Walton, J., & Jones, C. (2019). MOHC UKESM1.0-LL model output prepared for CMIP6 CMIP esm-piControl. *Earth System Grid Federation*. https://doi.org/10.22033/ESGF/CMIP6.5953

Tleuova, Z., Snow, D. D., Mukhamedzhanov, M., & Ermenbay, A. (2023). Relation of Hydrogeology and Contaminant Sources to Drinking Water Quality in Southern Kazakhstan. *Water*, 15(24), 4240. https://doi.org/10.3390/w15244240

United Nations Department of Economic and Social Affairs Population Division. (2022). World Population Prospects 2022 Demographic indicators by region, subregion and country, annually for 1950-2100 (27). *United Nations Department of Economic and Social Affairs, Population Division*.

Yukimoto, S., Koshiro, T., Kawai, H., Oshima, N., Yoshida, K., Urakawa, S., Tsujino, H., Deushi, M., Tanaka, T., Hosaka, M., Yoshimura, H., Shindo, E., Mizuta, R., Ishii, M., Obata, A., & Adachi, Y. (2019). MRI MRI-ESM2.0 model output prepared for CMIP6 CMIP historical. *Earth System Grid Federation*. https://doi.org/10.22033/ESGF/CMIP6.6842

Appendix

Table A1 lists the zonal parameters for the final calibrated hydrological model.

Table A1: Zonal parameter values of HBV models. These values are applied to 57 models in total. HBV model areas are not reported since they differ for all 57 models according to the geometry of the corresponding elevation band.

Param.	Unit	Zone A	Zone B	Zone M	Zone D
CFMax	mm/deg. C/d	3.9760632	3.7921795	6.5241363	4.5214644
CFR	-	0.1697879	0.051356	0.4999447	0.3057517
CWH	-	0.1	0.1194662	0.1199852	0.0809045
TT	deg. C	2.4312328	1.1763552	2.9998382	2.4312328
TTInt	deg. C	2	0.0025191	1.9992994	2
TTSM	deg. C	0	0.5799426	0.9998591	0
Beta	-	2.5	1	4.9978445	2.5
FC	m	0.25	0.0589636	0.65	0.25
PWP	-	0.5	0.9658056	0.0304671	0.0300558
SUMax	M	0.05	0.1	0.0628649	0.001031
Kr	1/d	0.05	0.05	0.2612245	0.0500067
Ku	1/d	0.01	0.01	0.0106188	0.0100046
Kl	1/d	0.0103699	0.0089935	0	0.016505
Kperc	1/d	0.3602316	0.3280102	0.7266497	0.3602316

Figure A1 shows seasonality diagnostics of the available gauge data. The diagnostics covers the 1979 – 1991 time period.

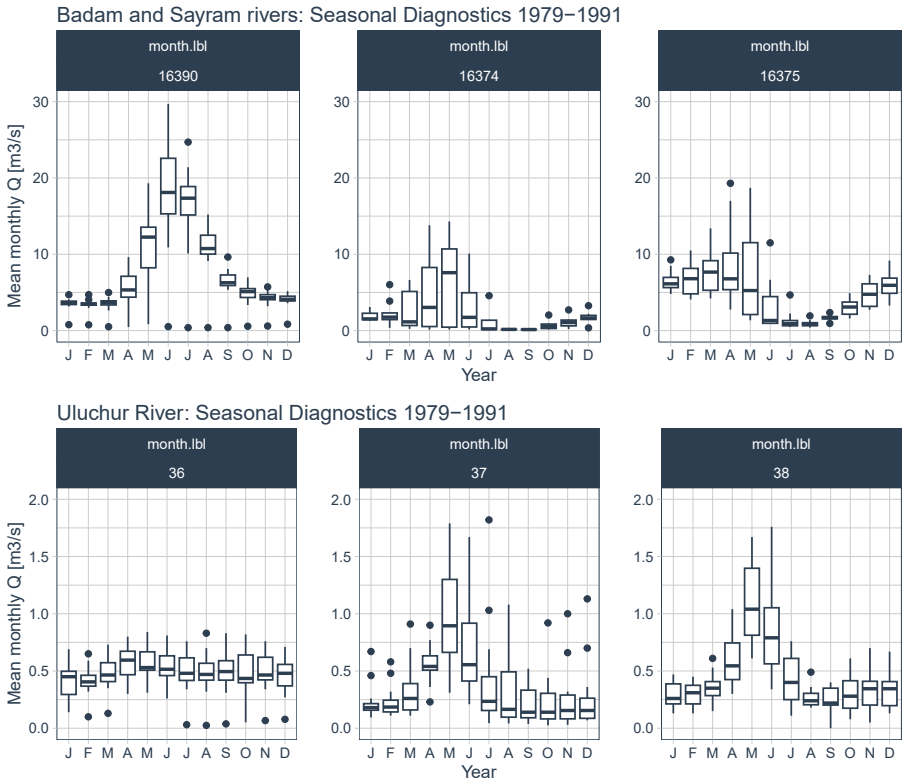

Figure A1: Seasonality diagnostics of river discharge. Compare with Figure 3 and Table 2 for a description of the gauge data and the time series plots. Uluchur river discharge peaks in May compared to Sayram River, which is a catchment with higher mean elevation and thus peaks only in June.

Figure A2 shows a screenshot of the RS MINERVE model.

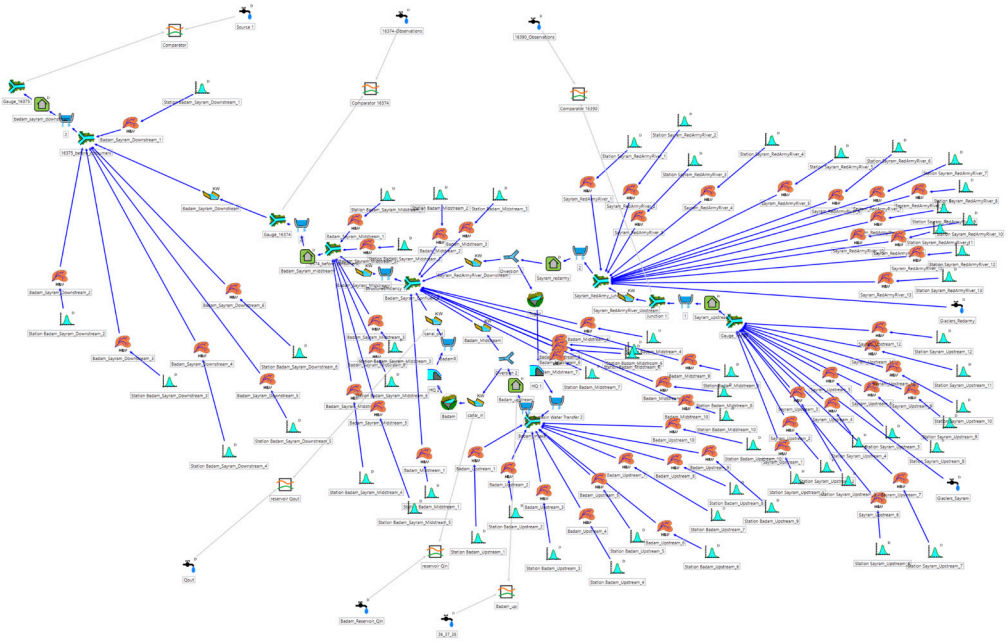

Figure A2: Screenshot of the RS MINERVE Badam semi-distributed conceptual hydrological model. The elevation basin and subbasin-specific HBV models are indicated in red. Elevation-bands-specific climate forcings are indicated by virtual meteorological stations in bright blue. The glacier contributions are computed externally and added via source terms (faucets). The blue arrows indicate the river routing directions connecting the individual hydrological models and hydraulic objects. Gauge locations are indicated by the comparator objects linked to location-specific structures.